



Grid-independent High Resolution Dust Emissions (v1.0) for Chemical Transport Models: Application to GEOS-Chem (version 12.5.0)

Jun Meng^{1,2}, Randall V. Martin^{2,1,3}, Paul Ginoux⁴, Melanie Hammer^{2,1}, Melissa P. Sulprizio⁵,

5 David A. Ridley⁶, Aaron van Donkelaar^{1,2}

¹Department of Physics and Atmospheric Science, Dalhousie University, Halifax, Nova Scotia, B3H 4R2, Canada

² Department of Energy, Environmental & Chemical Engineering, Washington University in St. Louis, St. Louis, Missouri 63130, United States

10 ³Smithsonian Astrophysical Observatory, Harvard-Smithsonian Center for Astrophysics, Cambridge, MA 02138, USA

⁴NOAA Geophysical Fluid Dynamics Laboratory, Princeton, New Jersey 08540, USA

⁵School of Engineering and Applied Science, Harvard University, Cambridge, MA 02138, USA

⁶California Environmental Protection Agency, Sacramento, CA 95814, USA

15

Correspondence to: Jun Meng (jun.meng@dal.ca)



Abstract. The nonlinear dependence of the dust saltation process on wind speed poses a
20 challenge for models of varying resolutions. This challenge is of particular relevance for the next
generation of chemical transport models with nimble capability for multiple resolutions. We
develop and apply a method to harmonize dust emissions across simulations of different
resolutions by generating offline grid independent dust emissions driven by native high
resolution meteorological fields. We implement into the GEOS-Chem chemical transport model
25 a high resolution dust source function to generate updated offline dust emissions. These
updated offline dust emissions based on high resolution meteorological fields can better
resolve weak dust source regions, such as in southern South America, southern Africa and the
southwestern United States. Identification of an appropriate dust emission strength is
facilitated by the resolution independence of offline emissions. We find that the performance
30 of simulated aerosol optical depth (AOD) versus measurements from the AERONET network
and satellite remote sensing improves significantly when using the updated offline dust
emissions with the total global annual dust emission strength of $2,000 \text{ Tg yr}^{-1}$ rather than the
standard online emissions in GEOS-Chem. The offline high resolution dust emissions are easily
implemented in chemical transport models. The source code is available online through GitHub:
35 <https://github.com/Jun-Meng/geos-chem/tree/v11-01-Patches-UniCF-vegetation>. The global
offline high resolution dust emission inventory is freely available (see Code and Data Availability
section).



1 Introduction

Mineral dust, as one of the most important natural aerosols in the atmosphere, has significant impacts on weather and climate by absorbing and scattering solar radiation (Bergin et al., 2017; Kosmopoulos et al., 2017), on atmospheric chemistry by providing surfaces for heterogeneous
45 reaction of trace gases (Chen et al., 2011; Tang et al., 2017), on the biosphere by fertilizing the tropical forest (Bristow et al., 2010; Yu et al., 2015), and on human health by increasing surface fine particulate matter (PM_{2.5}) concentrations (De Longueville et al., 2010; Fairlie et al., 2007; Zhang et al., 2013). Dust emissions are primarily controlled by surface wind speed, vegetation cover and soil water content. The principal mechanism for natural dust emission is saltation
50 bombardment (Gillette and Passi, 1988; Shao et al., 1993), in which sand-sized particles creep forward and initiate the suspension of smaller dust particles when the surface wind exceeds a threshold. The nonlinearity of this process introduces an artificial dependence of simulations upon model resolution (Ridley et al., 2013). For example, dust emissions in most numerical models are parameterized with an empirical method (e.g. Ginoux et al., 2001; Zender et al.,
55 2003), which requires a critical wind threshold to emit dust particles. Methods are needed to address the artificial dependence of simulations upon model resolution that arises from nonlinearity in dust emissions.

Addressing this nonlinearity is especially important for the next generation of chemistry transport models that is emerging with nimble capability for a variety of resolutions at the
60 global scale. For example, the high performance version of GEOS-Chem (GCHP) (Eastham et al., 2018) currently offers simulation resolutions from C24 (~ 4°x5°) to C360 (~0.25°), with progress toward even finer resolution and toward a variable stretched grid capability. Resolution-



dependent mineral dust emission would vary by a factor of 3 from C360 to C24, and inhibit interpretation (Ridley et al., 2013). Grid-independent high resolution dust emissions offer a
65 potential solution to this concern.

An important capability in global dust evaluation is ground-based and satellite remote sensing. The Aerosol Robotic Network (AERONET), a global ground-based remote sensing aerosol monitoring network of Sun photometers (Holben et al., 1998), has been widely used to evaluate dust simulations. Satellite remote sensing provides additional crucial information
70 across arid regions where in-situ observations are sparse (Hsu et al., 2013). Satellite aerosol retrievals have been used extensively in previous studies to either evaluate the dust simulation (Ridley et al., 2012, 2016) or constrain the dust emission budget (Zender et al., 2004). Satellite aerosol products have been used to identify dust sources worldwide (Ginoux et al., 2012; Schepanski et al., 2012; Yu et al., 2018), especially for small-scale sources (Gillette, 1999).

75 The objective of this study is to develop a method to mitigate the inconsistency of total dust emissions across different resolutions of simulations by generating and archiving an offline dust emission using native high resolution meteorological fields. We apply this method to the GEOS-Chem chemical transport model. As part of this effort, we implement an updated high resolution satellite-identified dust source function into the dust mobilization module of GEOS-
80 Chem to better represent the spatial structure of dust sources. We apply this new capability to assess the source strength that best represents observations.

2 Materials and Methods

2.1 Description of Observations



85 We use both ground-based and satellite observations to evaluate our GEOS-Chem simulations.
AERONET is a global ground-based remote sensing aerosol monitoring network of sun
photometers with direct sun measurements every 15 minutes (Holben et al., 1998). We use
Level 2.0 Version 3 data that has improved cloud screening algorithms (Giles et al., 2019).
Aerosol optical depth (AOD) at 550 nm is interpolated based on the local angstrom exponent at
90 the 440 nm and 670 nm channels.

Twin Moderate-Resolution Imaging Spectroradiometer (MODIS) instruments aboard
both on the Terra and Aqua NASA satellite platforms and provide near daily measurements
globally. We use the AOD at 550 nm retrieved from Collection 6.1 (C6) of MODIS product (Sayer
et al., 2014). We use AOD from the Deep Blue (DB) retrieval algorithm (Hsu et al., 2013; Sayer et
95 al., 2014) designed for bright surfaces, and the Multi-Angle Implementation of Atmospheric
Correction (MAIAC) algorithm (Lyapustin et al., 2018), which provides global AOD retrieved
from MODIS C6 radiances at a resolution of 1 km. The MAIAC AOD used in this study is
interpolated to the AOD value at 550 nm.

We compare the simulated fine AOD with measurements using reduced major axis
100 linear regression. We report root mean square error (E), correlation (R) and slope (M).

2.2 Dust mobilization module

We use the dust detrainment and deposition (DEAD) scheme (Zender et al., 2003) in the GEOS-
Chem model to calculate dust emission. The saltation process is dependent on the critical
105 threshold wind speed, which is determined by surface roughness, soil type and soil moisture.
We use a fixed soil clay fraction of 0.2 as suggested in Zender et al. (2003). Dust aerosol is



transported in four size bins (0.1-1.0, 1.0-1.8, 1.8-3.0, and 3.0-6.0 μm radius). Detailed description of the dust emission parameterization is in Sect. S1 of the supplemental material.

The fractional area of land with erodible dust is represented by a source function. The dust source function used in the dust emission module plays an important role in determining the spatial distribution of dust emissions. The standard GEOS-Chem model (version 12.5.0) uses a source function at $2^\circ \times 2.5^\circ$ resolution from Ginoux et al. (2001) as implemented by Fairlie et al. (2007). We implement an updated high resolution version of the dust source function in this study at $0.25^\circ \times 0.25^\circ$ resolution. Figure S1 shows a map of the original and updated version of the dust source function. The updated source function exhibits more spatially resolved information due to its finer spatial resolution resulting in a higher fraction of erodible dust over the eastern Arabian Peninsula, the Bodélé depression, and the central Asian deserts. The dust module dynamically applies this source function, together with information on soil moisture, vegetation, and land use to calculate hourly emissions using the HEMCO module described below.

2.3 Offline dust emissions at the native meteorological resolution

HEMCO (Keller et al., 2014) is a stand-alone software module for computing emissions in global atmospheric models. We run the HEMCO standalone version using native meteorological resolution ($0.25^\circ \times 0.3125^\circ$) data to archive the offline dust emissions at the same resolution as the meteorological data. In this study, we generate two offline dust emission datasets at $0.25^\circ \times 0.3125^\circ$ resolution. One, referred to as the default offline dust emissions, uses the existing dust source function in the dust module; the other, referred to as the updated offline dust



emissions, uses the updated dust source function implemented here. Both datasets are at the
130 hourly resolution of the parent meteorological fields. The archived native resolution offline dust
emissions can be an input emission inventory for chemical transport models with scalable dust
source strengths. We use the GEOS-Chem model to evaluate the dust simulations and the
emission strength.

135 **2.4 GEOS-Chem chemical transport model and simulation configurations**

GEOS-Chem (The International GEOS-Chem User Community, 2019) is a three-dimensional
chemical transport model driven by assimilated meteorological data from the Goddard Earth
Observation System (GEOS) of the NASA Global Modelling and Assimilation Office (GMAO). The
GEOS-Chem aerosol simulation includes the sulfate-nitrate-ammonium (SNA) aerosol system
140 (Fountoukis and Nenes, 2007; Park et al., 2004), carbonaceous aerosol (Hammer et al., 2016;
Park et al., 2003; Wang et al., 2014), secondary organic aerosols (Marais et al., 2016; Pye et al.,
2010), sea salt (Jaeglé et al., 2011) and mineral dust (Fairlie et al., 2007) with updates to aerosol
size distribution (Ridley et al., 2012; Zhang et al., 2013). Aerosol optical properties are based on
the Global Aerosol Data Set (GADS) as implemented by Martin et al. (2003) for externally mixed
145 aerosols as a function of local relative humidity with updates based on measurements (Drury et
al., 2010; Latimer and Martin, 2019). We include dry and wet deposition (Liu et al., 2001)
processes in the model. Gravitational settling for dust, is following Fairlie et al. (2007).

The original GEOS-Chem simulation used online dust emissions by coupling the dust
mobilization module online. We develop the capability to use offline dust emissions based on
150 the archived fields described in Sect. 2.3. We conduct global simulations with GEOS-Chem



(version 12.5.0) at a horizontal resolution of 2° by 2.5° for the year 2016. Simulations using the online and offline dust emissions are conducted to evaluate the offline dust emissions. We conduct two simulations using online dust emissions with different dust source functions. The first is with the original version of dust source function. The other one is with the updated
155 version of source function. The annual total emissions for the online dust emissions are at the original value of 909 Tg yr^{-1} . We conduct another two sets of simulations using offline dust emissions. The first uses the default offline dust emissions with the annual total dust emission of 909 Tg yr^{-1} . The second uses the updated offline dust emission with the annual total dust emission scaled to $2,000 \text{ Tg yr}^{-1}$, which is in the range of the current dust emission estimates of
160 over $426 - 2726 \text{ Tg yr}^{-1}$ (Huneeus et al., 2011) and better represents observations as will be shown below.

3 Results and Discussion

3.1 Spatial and seasonal variation of the offline dust emissions

165 Figure 1 shows the spatial distribution of the annual and seasonal dust emission flux rate for the updated offline dust emissions. The annual dust emission flux rate is high over major deserts, such as the northwestern Sahara, the Bodélé Depression in northern Chad, eastern Arabian Peninsula and central Asian Taklimakan and Gobi deserts. There are also hotspots of dust emission flux rate over relatively smaller deserts, such as the Mojave Desert of the
170 southwestern United States, the Atacama desert of southern South America, the Kalahari desert on the west coast of southern Africa and the deserts in central Australia. Those features reflect the fine resolution of the updated dust source function and of the offline dust emissions.



Seasonally, the dust emission flux rate resembles the annual distribution, however, with a lower dust emission flux rate over the Bodélé Depression in northern Chad in summer and higher dust emission flux rate over the Middle East and central Asian deserts in spring and summer.

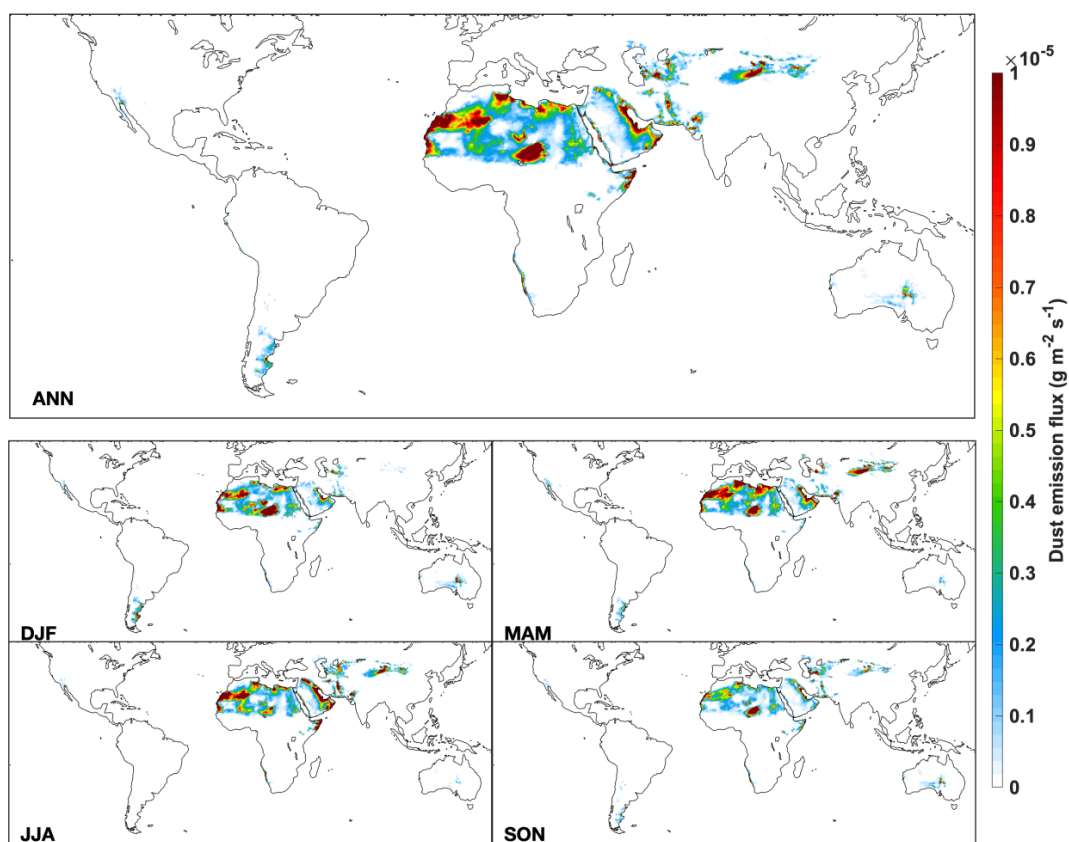
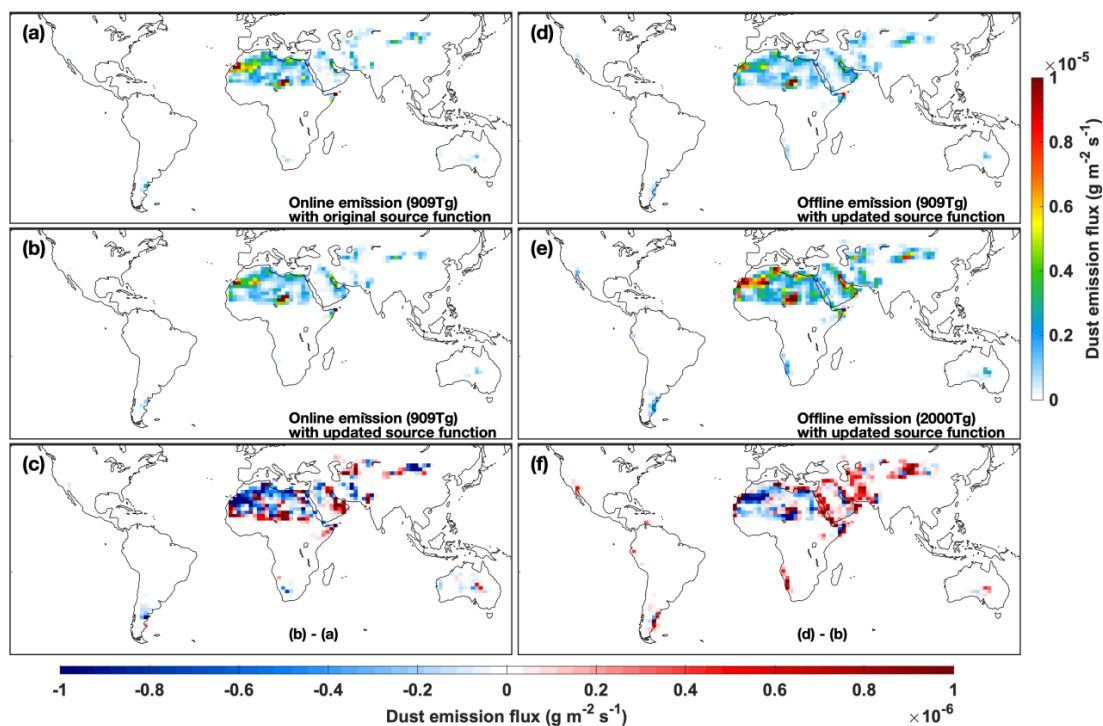


Figure 1. Annual and seasonal mean dust emission flux rate for the offline high resolution dust emissions with updated dust source function and updated annual total dust emission of 2,000 Tg.



180

Figure 2. Annual mean dust emission flux rate for 2016. (a), The original online dust emissions with original dust source function and annual total dust emissions of 909 Tg. (b), Online dust emissions with updated dust source function. (c), Difference of flux rate between online dust emissions using original and updated dust source functions. (d), Offline dust emissions with updated dust source function. (e), Offline dust emissions with updated dust source function and updated annual total dust emissions of 2,000 Tg. (f), Difference of flux rate between offline and online dust emissions. The online dust emissions are in $2^\circ \times 2.5^\circ$ resolution. The offline dust emissions shown in (b), (d), (f) are regridded from $0.25^\circ \times 0.3125^\circ$ resolution for comparison with online dust emissions.

185

Figure 2 shows the spatial distribution of the annual dust emission flux rate for the
190 online and offline dust emissions with the original and updated dust source functions with
original and updated global total dust source strengths. All simulations exhibit high dust
emission flux rates over major desert regions, such as the Sahara, Middle East and Central Asian
deserts, with local enhancements over the western Sahara and northern Chad. The simulation



with the updated source function exhibits stronger emissions in the Sahara and Persian Gulf
195 regions (Fig. 2c). The difference between the online and offline dust emissions, shown in Fig. 2f,
indicates that the offline dust emissions based on native resolution meteorological fields have
lower dust emission flux rates over northwest Africa, but higher dust emission flux rates over
the Middle East and Central Asia. Higher annual dust emission flux rates over the southwestern
United States, southern South America, west coast of southern Africa and central Australia in
200 the offline dust emissions reflect that the native resolution offline dust emissions are
strengthened over relatively weaker dust emission regions. Generally, coastal and minor desert
regions emit more dust when calculating emissions at the native meteorological resolution.

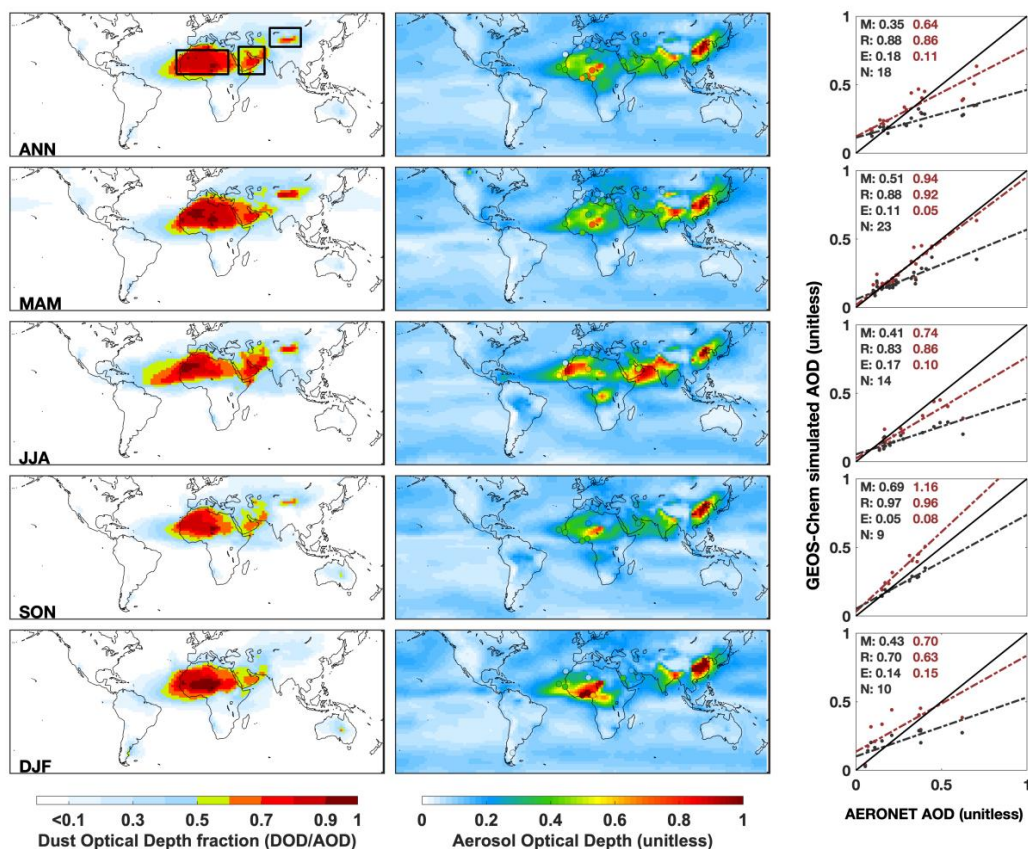
Figures S2–S5 show the seasonal variations of dust emission flux rates for online and
offline emissions. The offline dust emissions have lower emission flux rates than the online dust
205 emissions during spring (March, April and May) (MAM) and winter (December, January and
February) (DJF) over the Sahara Desert. The offline dust emission flux rate is higher than the
online dust emission flux rate over the Middle East and Central Asian deserts during spring and
summer (June, July and August) (JJA). Emission flux rates are low over Central Asian deserts
during winter. The strengthening of offline dust emissions over weaker dust emitting regions
210 persists throughout all seasons.

3.2 The performance of AOD simulations over desert regions

Figure 3 shows simulated AOD using the original online and updated offline dust emissions. We
select for evaluation the AERONET sites where the ratio of simulated dust optical depth (DOD)
215 to simulated total AOD exceeds 0.5 in the simulation using the updated offline dust emissions.



Annually, the simulated DOD has the highest value over the Bodélé Depression. This feature persists in all seasons except summer when DOD has the highest values over the western Sahara and eastern Arabian Peninsula. The scatter plots show that annually the simulated AOD from both simulations are highly correlated with AERONET measurements across the dust regions ($R = 0.86-0.88$). The simulation with updated offline dust emissions has an improved slope and smaller root mean square error than the simulation using the original online dust emissions. AOD from the simulation with updated offline dust emissions is also more consistent with the measurements in different seasons, especially in the spring (MAM) and fall (SON) with slopes close to unity and R exceeding 0.9.



225

230

Figure 3. Annual and seasonal mean simulated dust optical depth (DOD) fraction (left column) and aerosol optical depth (AOD) (middle column) from GEOS-Chem simulations for 2016, and AERONET measured AOD at sites where the ratio of simulated DOD and AOD exceeds 0.5, which are shown as filled circles in the middle column. Boxes in the left top panel outline the three major deserts examined in Figure 4. The right column shows the corresponding scatter plot with root mean square error (E), correlation coefficient (R) and slope (M) calculated with reduced major axis linear regression. N is the number of valid ground-based monitoring records. The results for the simulation using the original dust emissions are shown in black; the results for the simulation using updated dust emissions are shown in red. The best fit lines are dashed. The 1:1 line is solid.

235

We further evaluate the performance of simulated AOD over major desert regions using the MODIS Deep Blue (DB) and MAIAC AOD products. Figure 4 shows annual and seasonal scatter plots comparing GEOS-Chem simulated AOD using original online dust emissions and updated offline dust emissions against retrieved AOD from MODIS DB and MAIAC satellite



products over the three major desert regions outlined in Fig. 3. Figure S6 shows the annual and
240 seasonal AOD distribution from MODIS DB and MAIAC. Annually, the simulation using updated
offline dust emissions exhibits greater consistency with satellite AOD than does the simulation
using original online dust emissions across all three desert regions. The simulation using
updated offline dust emission performs better across all three desert regions and in all four
seasons except for the Sahara in summer, during which AOD is overestimated. Both simulations
245 underestimate AOD over central Asian deserts during winter when dust emissions are low and
other sources may be more important. Overall, the simulation using original online dust
emissions underestimates AOD over all three major desert regions, especially over the Middle
East and central Asian deserts. The simulation using updated offline dust emissions exhibits
greater consistency with satellite observations with higher slopes and correlations.

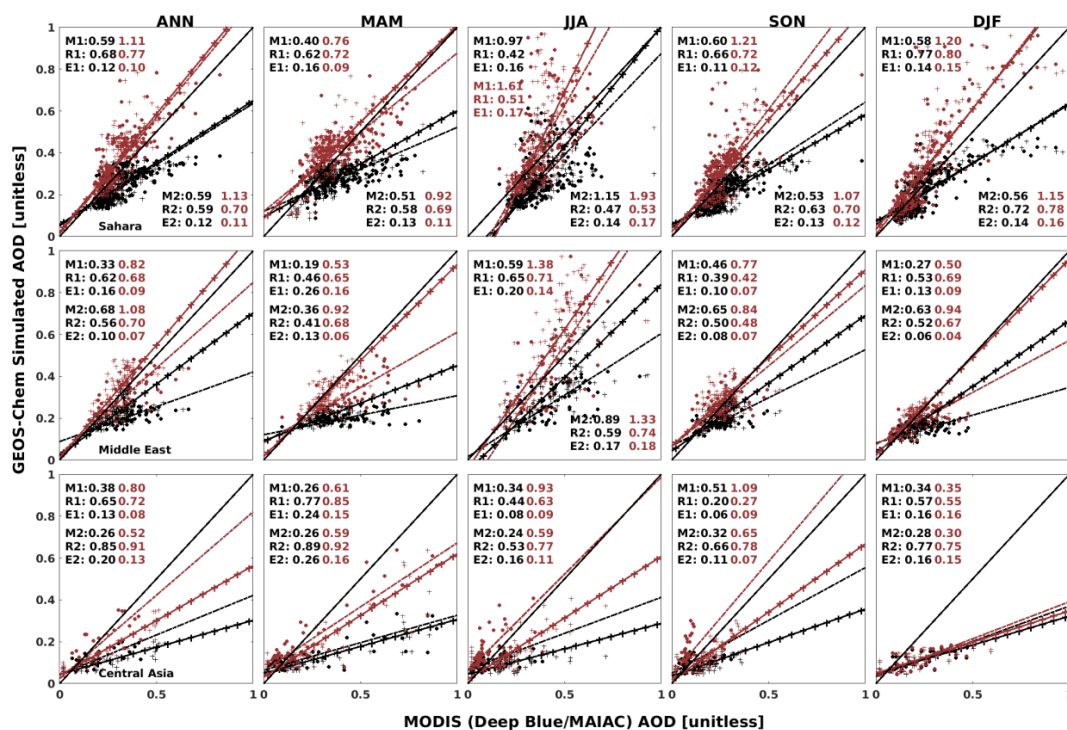
250

3.3 Discussion of the dust source strength

One of the advantages of the offline dust emissions is that the dust source strengths are
scalable. We have found that the simulation with global total annual dust emission scaled to
2,000 Tg better represents observations than does the default simulation with global total
255 annual dust emission of 909 Tg. We also evaluate simulations with global total annual dust
emission scaled to 1,500 Tg and 2,500 Tg. Figure S7 indicates that the simulation with global
total annual dust emission scaled to 2,000 Tg is more consistent with satellite observations over
the Sahara and Middle East. Although the central Asian deserts and regions with AERONET
observations (Fig. S8) are better represented by the simulation with global total annual dust
260 emission scaled to 2,500 Tg, since the Sahara has the highest dust emissions (Huneeus et al.,



2011), and AOD over the Sahara is most likely dominated by dust, we scale global total annual dust emissions to best match this source region. Additional development and evaluation should be conducted to further narrow the uncertainty of dust emissions, especially at the regional scale.



265

270

275

Figure 4. Scatter plots and statistics of comparing GEOS-Chem simulated AOD with satellite AOD over desert regions annually (the first column) and seasonally (the right four columns). The results for Sahara, Middle East and Central Asia deserts are shown in the top, middle and bottom rows respectively. The results for the simulation using the original dust emissions are shown in black; the results for the simulation using updated dust emissions are shown in red. Dots represent the comparison with MODIS Deep Blue AOD; the plus signs represent the comparison with MAIAC AOD. Correlation coefficient (R), root mean square error (E), and Slope (M) are reported, in which R1, E1 and M1 show the results of the comparison with MODIS Deep Blue AOD; R2, E2 and M2 show the results of the comparison with MAIAC AOD. The best fit lines are dashed lines with corresponding marker signs and colors. The 1:1 line solid black line.



3.4 Advantages of high resolution offline dust emissions for model development

Uncertainty remains in the estimated global annual total dust emissions. Direct dust emission
280 flux observations are few. Current atmospheric and chemical transport models apply a global
scale factor to optimize with a specific set of ground observations. Because of the non-linear
dependence on resolution of the dust emissions, the source strength has historically depended
upon model resolution, which inhibits general evaluation. The native resolution offline dust
emissions facilitate consistent evaluation and application across all model resolutions.

285

4 Summary and Conclusions

The nonlinear dependence of dust emission parameterizations upon model resolution poses a
challenge for the next generation of chemical transport models with nimble capability for
multiple resolutions. In this paper we have developed and tested a method to calculate offline
290 dust emissions at the native meteorological resolution to promote consistency of dust
emissions across different model resolutions. We take advantage of the capability of HEMCO
standalone module to calculate dust emission offline at native meteorological resolution using
DEAD dust emission scheme combined with an updated high resolution dust source function.
We evaluate the performance of the simulation with native resolution offline dust emissions
295 and an updated dust source function with source strength of $2,000 \text{ Tg yr}^{-1}$. We find better
agreement with measurements, including satellite and AERONET AOD. The offline fine
resolution dust emissions better resolve smaller desert regions. The independence of source
strength from simulation resolution facilitates evaluation with observations. Further work
should continue to develop and evaluate the representation of dust emissions.



300 **5 Code and Data Availability**

The source code for generating the offline dust emissions is available on GitHub

(<https://github.com/Jun-Meng/geos-chem/tree/v11-01-Patches-UniCF-vegetation>) and Zenodo repository (<https://doi.org/10.5281/zenodo.4062003>) (Meng et al., 2020b). The instruction of how to generate the emission files is in the README.md file in the GitHub repository

305 (<https://github.com/Jun-Meng/geos-chem/tree/v11-01-Patches-UniCF-vegetation>). The global high resolution (0.25°x0.3125°) dust emission inventory is available on Zenodo (<https://doi.org/10.5281/zenodo.4060248>) (Meng et al., 2020a), containing netCDF format files of global gridded hourly mineral dust emission flux rate. Currently, the dataset (version1.0) is available for the year 2016. The dataset for other years since 2014 will be available in future
310 versions.

The base GEOS-Chem source code in version 12.5.0 is available on Github

(<https://github.com/geoschem/geos-chem/tree/12.5.0>) and Zenodo repository (<https://zenodo.org/record/3403111#.X7PKv5NKiF0,%202019>). The GEOS-Chem simulation

315 output data and AOD observations used to evaluate the model performance, including MODIS Deep Blue, MODIS MAIAC and AERONET AOD, can be accessed via this Zenodo repository (<https://doi.org/10.5281/zenodo.4312944>) (Meng et al., 2020c).

Information about the Supplement

320 The supplement related to this article describes the details of the dust emission scheme used in this project, as well as additional figures described in the main text.



Author contributions

RVM and JM conceived the project. JM developed the dust emission dataset using data and
325 algorithms from DAR, PG, MH, AvD, and MPS. JM prepared the manuscript with contributions
from all coauthors. All authors helped revise the manuscript.

Competing interests

The authors declare that they have no conflict of interest.
330

Acknowledgement

This work was supported by the Natural Science and Engineering Research Council of Canada.
Jun Meng was partially supported by a Nova Scotia Research and Innovation Graduate
Scholarship. Martin acknowledges partial support from NASA AIST-18-0011. We are grateful to
335 Compute Canada and Research Infrastructure Services in Washington University in St. Louis for
computing resources. The meteorological data (GEOS-FP) used in this study have been provided
by the Global Modeling and Assimilation Office (GMAO) at NASA Goddard Space Flight Center.
All figures are produced with the MATLAB 2019a software.



340 References

- Bergin, M. H., Ghoroi, C., Dixit, D., Schauer, J. J. and Shindell, D. T.: Large Reductions in Solar Energy Production Due to Dust and Particulate Air Pollution, *Environ. Sci. Technol. Lett.*, 4(8), 339–344, doi:10.1021/acs.estlett.7b00197, 2017.
- Bristow, C. S., Hudson-Edwards, K. A. and Chappell, A.: Fertilizing the Amazon and equatorial
345 Atlantic with West African dust, *Geophysical Research Letters*, 37(14),
doi:10.1029/2010GL043486, 2010.
- Chen, H., Navea, J. G., Young, M. A. and Grassian, V. H.: Heterogeneous Photochemistry of Trace Atmospheric Gases with Components of Mineral Dust Aerosol, *J. Phys. Chem. A*, 115(4), 490–499, doi:10.1021/jp110164j, 2011.
- 350 De Longueville, F., Hountondji, Y.-C., Henry, S. and Ozer, P.: What do we know about effects of desert dust on air quality and human health in West Africa compared to other regions, *Sci. Total Environ.*, 409(1), 1–8, doi:10.1016/j.scitotenv.2010.09.025, 2010.
- Drury, E., Jacob, D. J., Spurr, R. J. D., Wang, J., Shinzuka, Y., Anderson, B. E., Clarke, A. D., Dibb, J., McNaughton, C. and Weber, R.: Synthesis of satellite (MODIS), aircraft (ICARTT), and surface
355 (IMPROVE, EPA-AQS, AERONET) aerosol observations over eastern North America to improve MODIS aerosol retrievals and constrain surface aerosol concentrations and sources, *Journal of Geophysical Research: Atmospheres*, 115(D14), doi:10.1029/2009JD012629, 2010.
- Eastham, S. D., Long, M. S., Keller, C. A., Lundgren, E., Yantosca, R. M., Zhuang, J., Li, C., Lee, C. J., Yannetti, M., Auer, B. M., Clune, T. L., Kouatchou, J., Putman, W. M., Thompson, M. A.,
360 Trayanov, A. L., Molod, A. M., Martin, R. V. and Jacob, D. J.: GEOS-Chem High Performance (GCHP v11-02c): a next-generation implementation of the GEOS-Chem chemical transport model for massively parallel applications, *Geoscientific Model Development*, 11(7), 2941–2953, doi:https://doi.org/10.5194/gmd-11-2941-2018, 2018.
- Fairlie, T. D., Jacob, D. J. and Park, R. J.: The impact of transpacific transport of mineral dust in
365 the United States, *Atmospheric Environment*, 41(6), 1251–1266,
doi:10.1016/j.atmosenv.2006.09.048, 2007.
- Fountoukis, C. and Nenes, A.: ISORROPIA II: A computationally efficient thermodynamic equilibrium model for K^+ - Ca^{2+} - Mg^{2+} - NH_4^+ - Na^+ - SO_4^{2-} - NO_3^- - Cl^- - H_2O aerosols, *Atmospheric Chemistry and Physics*, 7(17), 4639–4659, doi:https://doi.org/10.5194/acp-7-4639-2007, 2007.
- 370 Giles, D. M., Sinyuk, A., Sorokin, M. G., Schafer, J. S., Smirnov, A., Slutsker, I., Eck, T. F., Holben, B. N., Lewis, J. R., Campbell, J. R., Welton, E. J., Korokin, S. V. and Lyapustin, A. I.: Advancements in the Aerosol Robotic Network (AERONET) Version 3 database – automated near-real-time quality control algorithm with improved cloud screening for Sun photometer aerosol optical depth (AOD) measurements, *Atmospheric Measurement Techniques*, 12(1), 169–209,
375 doi:https://doi.org/10.5194/amt-12-169-2019, 2019.



- Gillette, D. A.: A qualitative geophysical explanation for hot spot dust emitting source regions, *Contrib. atmos. phys*, 72(1), 67–77, 1999.
- Gillette, D. A. and Passi, R.: Modeling dust emission caused by wind erosion, *Journal of Geophysical Research: Atmospheres*, 93(D11), 14233–14242, doi:10.1029/JD093iD11p14233, 1988.
- 380
- Ginoux, P., Chin, M., Tegen, I., Prospero, J. M., Holben, B., Dubovik, O. and Lin, S.-J.: Sources and distributions of dust aerosols simulated with the GOCART model, *Journal of Geophysical Research: Atmospheres*, 106(D17), 20255–20273, doi:10.1029/2000JD000053, 2001.
- Ginoux, P., Prospero, J. M., Gill, T. E., Hsu, N. C. and Zhao, M.: Global-scale attribution of anthropogenic and natural dust sources and their emission rates based on MODIS Deep Blue aerosol products, *Reviews of Geophysics*, 50(3), doi:10.1029/2012RG000388, 2012.
- 385
- Hammer, M. S., Martin, R. V., van Donkelaar, A., Buchard, V., Torres, O., Ridley, D. A. and Spurr, R. J. D.: Interpreting the ultraviolet aerosol index observed with the OMI satellite instrument to understand absorption by organic aerosols: implications for atmospheric oxidation and direct radiative effects, *Atmospheric Chemistry and Physics*, 16(4), 2507–2523, doi:https://doi.org/10.5194/acp-16-2507-2016, 2016.
- 390
- Holben, B. N., Eck, T. F., Slutsker, I., Tanré, D., Buis, J. P., Setzer, A., Vermote, E., Reagan, J. A., Kaufman, Y. J., Nakajima, T., Lavenu, F., Jankowiak, I. and Smirnov, A.: AERONET—A Federated Instrument Network and Data Archive for Aerosol Characterization, *Remote Sensing of Environment*, 66(1), 1–16, doi:10.1016/S0034-4257(98)00031-5, 1998.
- 395
- Hsu, N. C., Jeong, M.-J., Bettenhausen, C., Sayer, A. M., Hansell, R., Seftor, C. S., Huang, J. and Tsay, S.-C.: Enhanced Deep Blue aerosol retrieval algorithm: The second generation, *Journal of Geophysical Research: Atmospheres*, 118(16), 9296–9315, doi:10.1002/jgrd.50712, 2013.
- Huneeus, N., Schulz, M., Balkanski, Y., Griesfeller, J., Prospero, J., Kinne, S., Bauer, S., Boucher, O., Chin, M., Dentener, F., Diehl, T., Easter, R., Fillmore, D., Ghan, S., Ginoux, P., Grini, A., Horowitz, L., Koch, D., Krol, M. C., Landing, W., Liu, X., Mahowald, N., Miller, R., Morcrette, J.-J., Myhre, G., Penner, J., Perlwitz, J., Stier, P., Takemura, T. and Zender, C. S.: Global dust model intercomparison in AeroCom phase I, *Atmospheric Chemistry and Physics*, 11(15), 7781–7816, doi:https://doi.org/10.5194/acp-11-7781-2011, 2011.
- 400
- Jaeglé, L., Quinn, P. K., Bates, T. S., Alexander, B. and Lin, J.-T.: Global distribution of sea salt aerosols: new constraints from in situ and remote sensing observations, *Atmospheric Chemistry and Physics*, 11(7), 3137–3157, doi:https://doi.org/10.5194/acp-11-3137-2011, 2011.
- 405
- Keller, C. A., Long, M. S., Yantosca, R. M., Da Silva, A. M., Pawson, S. and Jacob, D. J.: HEMCO v1.0: a versatile, ESMF-compliant component for calculating emissions in atmospheric models, *Geoscientific Model Development*, 7(4), 1409–1417, doi:https://doi.org/10.5194/gmd-7-1409-2014, 2014.
- 410



- 415 Kosmopoulos, P. G., Kazadzis, S., Taylor, M., Athanasopoulou, E., Speyer, O., Raptis, P. I.,
Marinou, E., Proestakis, E., Solomos, S., Gerasopoulos, E., Amiridis, V., Bais, A. and Kontoes, C.:
Dust impact on surface solar irradiance assessed with model simulations, satellite observations
and ground-based measurements, *Atmospheric Measurement Techniques*, 10(7), 2435–2453,
doi:<https://doi.org/10.5194/amt-10-2435-2017>, 2017.
- Latimer, R. N. C. and Martin, R. V.: Interpretation of measured aerosol mass scattering
efficiency over North America using a chemical transport model, *Atmospheric Chemistry and
Physics*, 19(4), 2635–2653, doi:<https://doi.org/10.5194/acp-19-2635-2019>, 2019.
- 420 Liu, H., Jacob, D., Bey, I. and Yantosca, R.: Constraints from ²¹⁰Pb and ⁷Be on wet deposition
and transport in a global three-dimensional chemical tracer model driven by assimilated
meteorological fields, *Journal of Geophysical Research: Atmospheres*, 106,
doi:10.1029/2000JD900839, 2001.
- Lyapustin, A., Wang, Y., Korkin, S. and Huang, D.: MODIS Collection 6 MAIAC algorithm,
425 *Atmospheric Measurement Techniques*, 11(10), 5741–5765, doi:<https://doi.org/10.5194/amt-11-5741-2018>, 2018.
- Marais, E. A., Jacob, D. J., Jimenez, J. L., Campuzano-Jost, P., Day, D. A., Hu, W., Krechmer, J.,
Zhu, L., Kim, P. S., Miller, C. C., Fisher, J. A., Travis, K., Yu, K., Hanisco, T. F., Wolfe, G. M.,
Arkinson, H. L., Pye, H. O. T., Froyd, K. D., Liao, J. and McNeill, V. F.: Aqueous-phase mechanism
430 for secondary organic aerosol formation from isoprene: Application to the southeast United
States and co-benefit of SO₂ emission controls, *Atmospheric Chemistry and Physics*, 16(3),
1603–1618, doi:<https://doi.org/10.5194/acp-16-1603-2016>, 2016.
- Martin, R. V., Jacob, D. J., Yantosca, R. M., Chin, M. and Ginoux, P.: Global and regional
decreases in tropospheric oxidants from photochemical effects of aerosols, *Journal of
435 Geophysical Research: Atmospheres*, 108(D3), doi:10.1029/2002JD002622, 2003.
- Meng, J., Martin, R. V., Ginoux, P., Ridley, D. A. and Sulprizio, M. P. : Global High Resolution
Dust Emission Inventory for Chemical Transport Models, Zenodo,
<https://doi.org/10.5281/zenodo.4060248>, 2020.
- 440 Meng, J., Martin, R. V. and Ridley, D. A.: Offline_Dust_Emissions_SourceCode_2020_v1.0.,
Zenodo, <https://doi.org/10.5281/zenodo.4062003>, 2020.
- Meng, J., Martin, R. V., Hammer, M., van Donkelaar, A., Ginoux, P., and Ridley, D. A.:
Observations of AOD and GEOS-Chem simulation model output dataset, Zenodo,
<https://doi.org/10.5281/zenodo.4312944>, 2020.
- 445 Park, R. J., Jacob, D. J., Chin, M. and Martin, R. V.: Sources of carbonaceous aerosols over the
United States and implications for natural visibility, *Journal of Geophysical Research:
Atmospheres*, 108(D12), 4355, doi:10.1029/2002JD003190, 2003.



- 450 Park, R. J., Jacob, D. J., Field, B. D., Yantosca, R. M. and Chin, M.: Natural and transboundary pollution influences on sulfate-nitrate-ammonium aerosols in the United States: Implications for policy, *Journal of Geophysical Research: Atmospheres*, 109(D15), doi:10.1029/2003JD004473, 2004.
- Pye, H. O. T., Chan, A. W. H., Barkley, M. P. and Seinfeld, J. H.: Global modeling of organic aerosol: The importance of reactive nitrogen (NO_x and NO₃), *Atmospheric Chemistry and Physics*, 10(22), 11261–11276, doi:https://doi.org/10.5194/acp-10-11261-2010, 2010.
- 455 Ridley, D. A., Heald, C. L. and Ford, B.: North African dust export and deposition: A satellite and model perspective, *Journal of Geophysical Research: Atmospheres*, 117(D2), doi:10.1029/2011JD016794, 2012.
- Ridley, D. A., Heald, C. L., Pierce, J. R. and Evans, M. J.: Toward resolution-independent dust emissions in global models: Impacts on the seasonal and spatial distribution of dust, *Geophysical Research Letters*, 40(11), 2873–2877, doi:10.1002/grl.50409, 2013.
- 460 Ridley, D. A., Heald, C. L., Kok, J. F. and Zhao, C.: An observationally constrained estimate of global dust aerosol optical depth, *Journal of Geophysical Research: Atmospheres*, 16(23), 15097–15117, doi:10.5194/acp-16-15097-2016, 2016.
- Sayer, A. M., Munchak, L. A., Hsu, N. C., Levy, R. C., Bettenhausen, C. and Jeong, M.-J.: MODIS Collection 6 aerosol products: Comparison between Aqua's e-Deep Blue, Dark Target, and "merged" data sets, and usage recommendations, *Journal of Geophysical Research: Atmospheres*, 119(24), 13,965–13,989, doi:10.1002/2014JD022453, 2014.
- 465 Schepanski, K., Tegen, I. and Macke, A.: Comparison of satellite based observations of Saharan dust source areas, *Remote Sensing of Environment*, 123, 90–97, doi:10.1016/j.rse.2012.03.019, 2012.
- 470 Shao, Y., Raupach, M. R. and Findlater, P. A.: Effect of saltation bombardment on the entrainment of dust by wind, *Journal of Geophysical Research: Atmospheres*, 98(D7), 12719–12726, doi:10.1029/93JD00396, 1993.
- Tang, M., Huang, X., Lu, K., Ge, M., Li, Y., Cheng, P., Zhu, T., Ding, A., Zhang, Y., Gligorovski, S., Song, W., Ding, X., Bi, X. and Wang, X.: Heterogeneous reactions of mineral dust aerosol: implications for tropospheric oxidation capacity, *Atmospheric Chemistry and Physics*, 17(19), 11727–11777, doi:https://doi.org/10.5194/acp-17-11727-2017, 2017.
- 475 The International GEOS-Chem User Community: geoschem/geos-chem: GEOS-Chem 12.5.0 (Version 12.5.0), Zenodo, <https://zenodo.org/record/3403111#.X7PKv5NKiF0>, 2019.
- 480 Wang, Q., Jacob, D. J., Spackman, J. R., Perring, A. E., Schwarz, J. P., Moteki, N., Marais, E. A., Ge, C., Wang, J. and Barrett, S. R. H.: Global budget and radiative forcing of black carbon aerosol: Constraints from pole-to-pole (HIPPO) observations across the Pacific, *Journal of Geophysical Research: Atmospheres*, 119, 195–206, doi:10.1002/2013JD020824, 2014.



- 485 Yu, H., Chin, M., Yuan, T., Bian, H., Remer, L. A., Prospero, J. M., Omar, A., Winker, D., Yang, Y.,
Zhang, Y., Zhang, Z. and Zhao, C.: The fertilizing role of African dust in the Amazon rainforest: A
first multiyear assessment based on data from Cloud-Aerosol Lidar and Infrared Pathfinder
Satellite Observations, *Geophysical Research Letters*, 42(6), 1984–1991,
doi:10.1002/2015GL063040, 2015.
- 490 Yu, Y., Kalashnikova, O. V., Garay, M. J., Lee, H. and Notaro, M.: Identification and
Characterization of Dust Source Regions Across North Africa and the Middle East Using MISR
Satellite Observations, *Geophysical Research Letters*, 45(13), 6690–6701,
doi:10.1029/2018GL078324, 2018.
- Zender, C. S., Bian, H. and Newman, D.: Mineral Dust Entrainment and Deposition (DEAD)
model: Description and 1990s dust climatology, *Journal of Geophysical Research: Atmospheres*,
108(D14), doi:10.1029/2002JD002775, 2003.
- 495 Zender, C. S., Miller, R. L. R. L. and Tegen, I.: Quantifying mineral dust mass
budgets: Terminology, constraints, and current estimates, *Eos, Transactions American
Geophysical Union*, 85(48), 509–512, doi:10.1029/2004EO480002, 2004.
- 500 Zhang, L., Kok, J. F., Henze, D. K., Li, Q. and Zhao, C.: Improving simulations of fine dust surface
concentrations over the western United States by optimizing the particle size distribution,
Geophysical Research Letters, 40(12), 3270–3275, doi:10.1002/grl.50591, 2013.